Materials Today Catalysis 5 (2024) 100053

Contents lists available at ScienceDirect

Materials Today Catalysis

journal homepage: www.journals.elsevier.com/materials-today-catalysis

Effect of β-fluorinated porphyrin in changing selectivity for electrochemical O_2 reduction

Ashwin Chaturvedi [a,1], Sandeep Dash [b,1], Soumalya Sinha [a], Julien A. Panetier [b,*], Jianbing Jiang (Jimmy)[a,*]

[a] Department of Chemistry, University of Cincinnati, P.O. Box 210172, Cincinnati, OH 45221, United States
[b] Department of Chemistry, State University of New York at Binghamton, Binghamton, NY 13902 United States

ARTICLE INFO

Keywords:
O_2 reduction reaction (ORR)
Homogeneous electrocatalysis
Cobalt
Fluorination
Porphyrins
Density functional theory

ABSTRACT

The development of catalytic systems that selectively convert O_2 to water is required to progress fuel cell technology. As an alternative to platinum catalysts, derivatives of iron and cobalt porphyrin molecular catalysts provide one benchmark for catalyst design. However, the inclusion of these catalysts into homogeneous platforms remains a difficulty. Co-porphyrins have been studied as heterogeneous O_2 reduction catalysts; however, they have not been explored much in homogeneous systems. Moreover, they suffer from poor selectivity for the desired four-electron reduction of O_2 to H_2O. Herein, we present two cobalt-based β-fluorinated porphyrin complexes (**$CoTPF_8(OH)_2$** and **$CoTPF_8(OH)_4$**) and demonstrate applicability as effective catalysts for the oxygen reduction reaction. Using rotating ring-disk electrochemistry, the catalysts, **$CoTPF_8(OH)_2$** and **$CoTPF_8(OH)_4$**, showed maximum Faradaic efficiency for H_2O of 92 % and 97 %, respectively. DFT calculations suggest that the formation of a phlorin intermediate could occur before O_2 reduction and that a stronger H_2O_2 binding in the cobalt-based β-fluorinated porphyrin species compared to the unsubstituted parent compound, **$CoTP(OH)_2$**, was responsible for the observed experimental selectivity for H_2O. These results reveal that the β-fluorinated porphyrin catalyst serves as a novel platform for investigating molecular electrocatalytic reactions.

1. Introduction

Oxygen reduction reaction (ORR) is important in various biological processes and technologies used in energy storage [1,2]. O_2 is either reduced by two electrons to form hydrogen peroxide (H_2O_2) or reduced by four electrons to form H_2O. These products of ORR either retain the O—O bond to produce H_2O_2 or cleave the O—O bond to form H_2O. Although H_2O_2 is vital to many industrial processes, it is an undesirable product as it can degrade both the membranes and biomolecules used in fuel cells and has a lower cell voltage [3]. Consequently, there is great interest in understanding the development of selective catalysts for four-proton, four-electron reduction of O_2 to H_2O [4]. O_2 reduction catalysts have sluggish kinetics and suffer from the formation of partially reduced products such as $O_2^{\bullet-}$ or H_2O_2 [5]. Therefore, the need for precious metal catalysts adds to the technological and socioeconomic problems that renewable technologies face.

Metalloporphyrins are significant molecules for oxygen binding and activation chemistry because of their ability to coordinate with a wide range of metal ions and create metal-oxygen complexes. These complexes are involved in various biological and chemical processes, including the transport of oxygen in hemoglobin and the activation of oxygen in catalytic reactions. Iron (Fe) porphyrins with an axial histidine imidazole group catalyze the selective reduction of O_2 to water in cytochrome c oxidase (CcO) [6–8]. Using an electronic "push effect," the axial imidazole group can raise the electron density of Fe and, thus, promote O_2 binding and activation at the Fe core.

In addition to biologically relevant Fe porphyrins, cobalt (Co) porphyrins are among the most extensively studied molecular catalysts for the oxygen reduction reaction (ORR) [9–13]. Cao and coworkers reported a Co porphyrin with an imidazole group attached to the porphyrin backbone for Co axial binding as an active bifunctional electrocatalyst for oxygen reduction and showed the importance of using axial ligands in enhancing ORR [14]. Anson and co-workers demonstrated that adsorption of cobalt [15–17] on carbon electrodes

* Corresponding authors.
E-mail addresses: panetier@binghamton.edu (J.A. Panetier), jianbing.jiang@uc.edu (J. Jiang).
[1] The authors contributed equally.

https://doi.org/10.1016/j.mtcata.2024.100053
Received 28 March 2024; Received in revised form 30 April 2024; Accepted 18 May 2024
Available online 22 May 2024

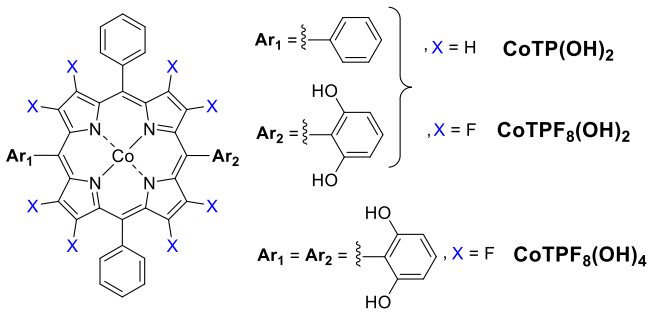

Scheme 1. Structures of the cobalt complexes in this work.

Table 1
Summary of electrochemical data for **$CoTP(OH)_2$**, **$CoTPF_8(OH)_2$**, and **$CoTPF_8(OH)_4$**.

Complex	$E_{1/2}$ for the first redox event (V vs. Fc/Fc^+)
$CoTP(OH)_2$	– 1.36
$CoTPF_8(OH)_2$	– 0.97
$CoTPF_8(OH)_4$	– 1.01

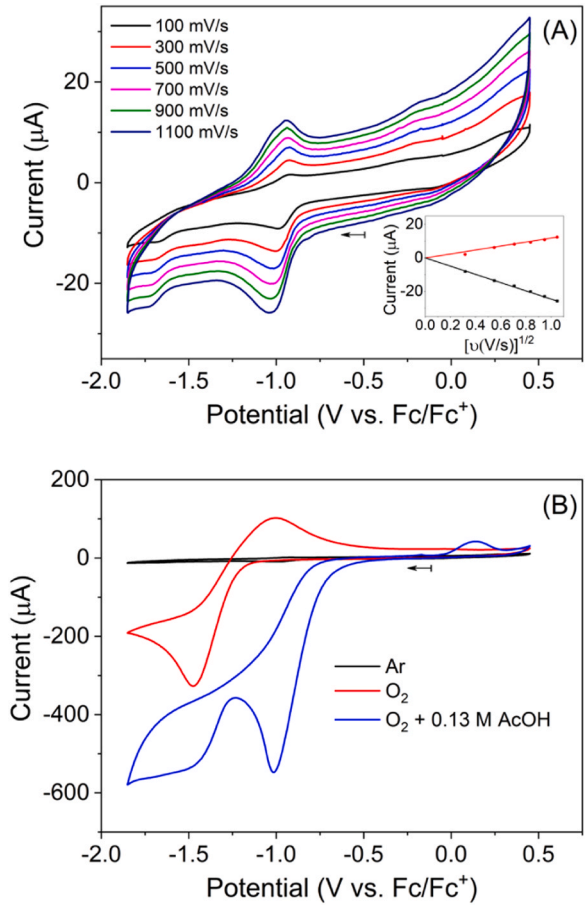

Fig. 1. Cyclic voltammograms (CV) of (A) Scan-rate-dependent cyclic voltammetry of 1.0 mM **$CoTPF_8(OH)_2$** in 0.1 M $TBAPF_6$/MeCN. Inset: Square root of scan rate vs. current for the first redox event. The R^2 value for the linear fit is 0.99. (B) Comparative CVs recorded for **$CoTPF_8(OH)_2$** in Ar- saturated (black) 0.1 M $TBAPF_6$/MeCN, O_2- saturated (red) 0.1 M $TBAPF_6$/MeCN, and after the addition of 0.13 M AcOH (blue) in O_2- saturated 0.1 M $TBAPF_6$/MeCN. All CVs were recorded at a 0.1 V/s scan rate.

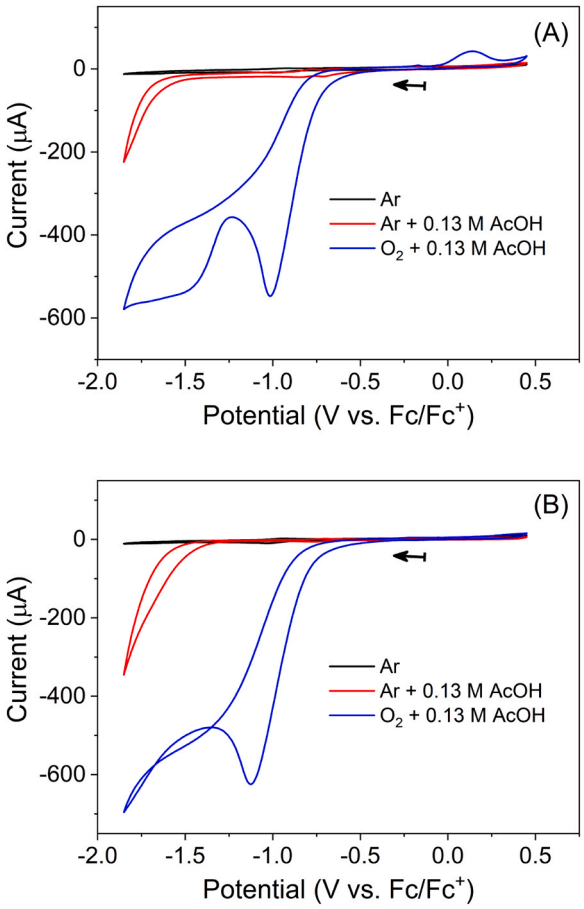

Fig. 2. Comparative CVs recorded for (A) **$CoTPF_8(OH)_2$** in Ar- (red) and O_2-saturated (blue) 0.1 M $TBAPF_6$/MeCN in the presence of 0.13 M AcOH. (B) **$CoTPF_8(OH)_4$** in Ar- (red) and O_2- saturated (blue) 0.1 M $TBAPF_6$/MeCN in the presence of 0.13 M AcOH. All CVs were recorded at a 0.1 V/s scan rate.

also gives rise to ORR chemistry. However, many Co-porphyrins produce H_2O_2 as the primary reaction product in O_2 reduction. Warren and coworkers demonstrated the importance of electrostatic interactions and proton relay activity of pendant groups in ORR catalysis [18]. The authors showed that the Co porphyrin with cationic ancillary group can stabilize intermediates through electrostatic interactions, which is essential in improving the selectivity for the $4H^+/4e^-$ reduction of O_2 to H_2O. Cao and coworkers showed that the ORR selectivity of Co porphyrins can be controlled by tuning steric effects [4]. The authors prepared several atropisomers of picket fence Co porphyrin and revealed that the atropisomers show distinct ORR selectivity due to the steric hindrances formed by functional groups' orientations. Co-porphyrins have been studied mainly as ORR catalysts by displaying high activity but poor selectivity towards H_2O [11].

In this study, we present the synthesis as well as the electrochemical and catalytic properties of cobalt-based β-fluorinated porphyrin complexes (**$CoTPF_8(OH)_2$** and **$CoTPF_8(OH)_4$**) and demonstrate its applicability as an effective catalyst for ORR. A combination of spectroscopy and voltammetry was employed to evaluate the catalytic efficiency and propose the catalytic mechanism for O_2 evolution. The redox and catalytic properties of the control compound, one without the β-fluorinated substituents, **$CoTP(OH)_2$**, were also investigated to provide insights into the structure-function relationship.

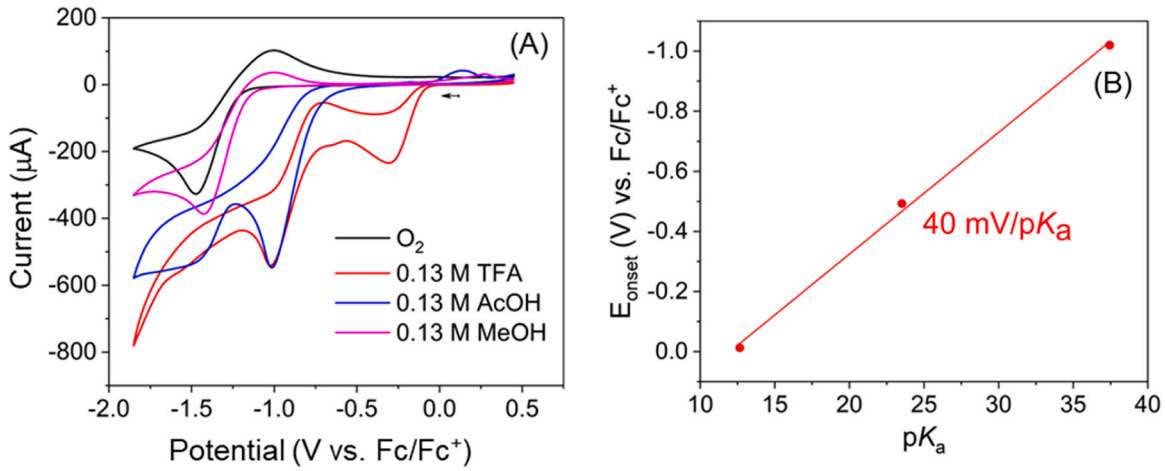

Fig. 3. (A) CVs recorded for **$CoTPF_8(OH)_2$** in O_2- saturated MeCN in the absence of any acid (black) and the presence of 0.13 M concentration of TFA (red), AcOH (blue), and MeOH (pink). (B) Onset potentials, E_{onset} (V), produced from (A), plotted vs. the pKa values of the corresponding acids in MeCN. The R^2 value for the linear fit is 0.99.

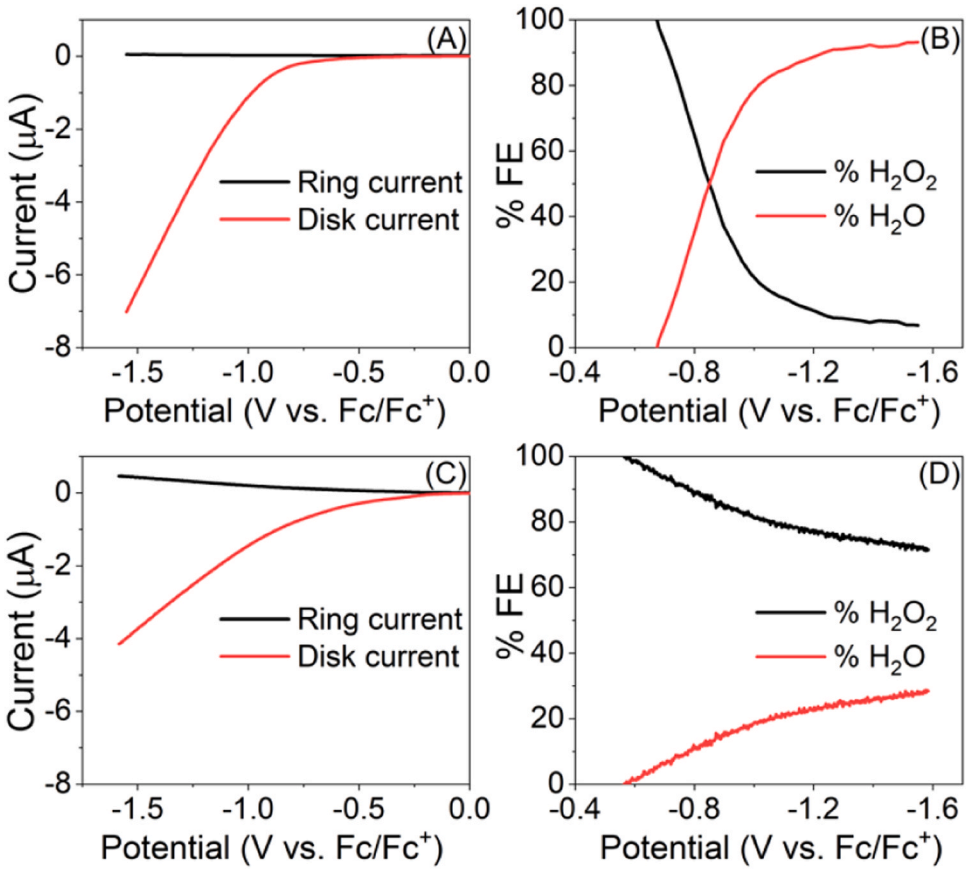

Fig. 4. (A) RRDE data for **$CoTPF_8(OH)_2$** (1.0 mM) in O_2- saturated 0.1 M $TBAPF_6$/MeCN with 0.13 M AcOH at the rotation rate of 300 rpm. Scan rate = 0.02 V/s. The potential at the Pt ring was held at 0.9 V vs. Fc/Fc^+. (B) Faradaic efficiencies (% FE) for H_2O_2 and H_2O obtained from the data, as shown in (A) by using Eq. (1). (C) RRDE data for **$CoTP(OH)_2$** (1.0 mM) in O_2- saturated 0.1 M $TBAPF_6$/MeCN with 0.13 M AcOH at the rotation rate of 300 rpm. Scan rate = 0.02 V/s. The potential at the Pt ring was held at 0.9 V vs. Fc/Fc^+. (D) Faradaic efficiencies for H_2O_2 and H_2O obtained from the data, as shown in (C) by using Eq. (1).

2. Results and discussion

2.1. Synthesis and characterization

Two β-fluorinated porphyrin complexes, **$CoTPF_8(OH)_2$** and **$CoTPF_8(OH)_4$** (Scheme 1), were prepared for electrocatalytic oxygen reduction. The preparation of both compounds involves a multi-step synthesis that starts with the introduction of the fluorine atoms to the beta-position of the pyrrole rings, followed by the synthesis of the porphyrin core with hydroxy groups at the ortho-positions, and then the cobalt metalation of the corresponding free-base porphyrin ligand (Scheme S1–S3). The β-substitution of the porphyrin with fluorine atoms (1) significantly modifies the electronic properties of the porphyrin ring, leading to tunable reactivity, and (2) affects the redox properties of the

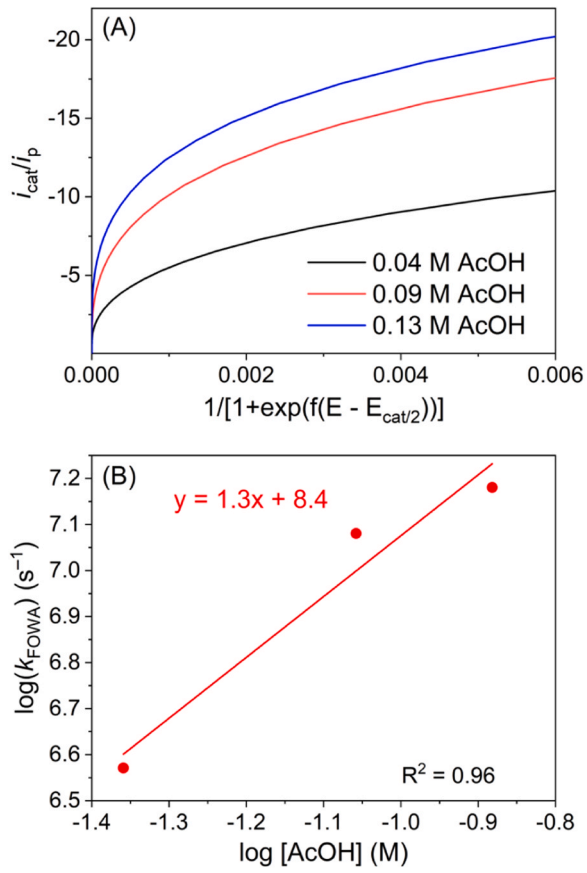

Fig. 5. (A) Fitting of the FOWA equation for the CVs of **CoTPF$_8$(OH)$_2$** in O_2-saturated MeCN in the presence of different concentrations of AcOH, 0.04 M (black), 0.09 M (red), and 0.13 M (blue). (B) Plot for the logarithm of k_{FOWA}, as estimated from the FOWA vs. the logarithm of AcOH concentration and fitted linearly.

molecule by decreasing the reduction potential [19–21]. The **CoTPF$_8$(OH)$_2$** and **CoTPF$_8$(OH)$_4$** catalysts were prepared by dissolving the corresponding free-base porphyrin ligand in chloroform and mixing with a solution of cobalt (II) acetate tetrahydrate (10 equiv.) in methanol. The mixture was stirred at a temperature of 50 °C for 12 h, and the progress of the reaction was monitored by thin-layer chromatography (TLC).

All three target compounds, **CoTP(OH)$_2$**, **CoTPF$_8$(OH)$_2$**, and **CoTPF$_8$(OH)$_4$**, were purified and characterized by UV–visible spectroscopy, matrix-assisted laser desorption/ionization (MALDI) mass spectroscopy, and high-resolution mass spectrometry (HR-MS) before the electrochemical and catalysis studies (Figs. S1–S11).

2.2. Electrochemical studies

2.2.1. Cyclic voltammetry studies under Ar

The electrochemical properties of the compounds **CoTP(OH)$_2$**, **CoTPF$_8$(OH)$_2$**, and **CoTPF$_8$(OH)$_4$** were studied by cyclic voltammetry (CV) measurements in anhydrous MeCN with 0.1 M tetrabutylammonium hexafluorophosphate ($TBAPF_6$) containing 1.0 mM of catalyst in an argon atmosphere. CV analysis of **CoTP(OH)$_2$**, **CoTPF$_8$(OH)$_2$**, and **CoTPF$_8$(OH)$_4$** reveal that the three cobalt complexes show a quasi-reversible feature (Table 1). These potentials at approximately − 1.00 V vs. Fc/Fc^+ are assigned to ligand-based redox events based on DFT calculations (*vide infra*). The presence of the fluorine on the β-positions of the porphyrin macrocycle shifts the potentials more positively ($\Delta E_{1/2}$ = 390 mV). CVs were also performed for **CoTP(OH)$_2$**, **CoTPF$_8$(OH)$_2$**, and **CoTPF$_8$(OH)$_4$** in Ar-saturated MeCN at different scan rates (100–1100 mV/s, Fig. 1A and Figs. S12–S13), and a linear relationship between cathodic peak current for the first redox event and the square root of the scan rate (Fig. 1A inset) indicates a diffusion-controlled process according to the Randles–Sevcik equation with no significant deposition or adsorption of molecules onto the electrode surface [22].

2.2.2. Homogeneous electrochemical ORR in the presence of AcOH to deduce the rate constant

In the presence of 0.13 M AcOH, the CVs of **CoTPF$_8$(OH)$_2$** and **CoTPF$_8$(OH)$_4$** in O_2-saturated MeCN showed an increase in current density at the peak potential of the first redox event and moved the peak potential towards more positive potentials (Fig. 1B and Fig. S14). For the O_2-saturated MeCN solution of **CoTPF$_8$(OH)$_2$** and **CoTPF$_8$(OH)$_4$** in the presence of 0.13 M AcOH, a catalytic peak current density of 8.3 mA/cm^2 and 8.8 mA/cm^2 respectively was measured at a potential of – 1.0 V vs. Fc/Fc^+ (Fig. 1B, blue line). This current density is comparatively higher and occurs at a lower negative potential than those observed for the glassy carbon (GC) electrode in the absence of 0.13 M AcOH [23]. A control experiment for **CoTPF$_8$(OH)$_2$** and **CoTPF$_8$(OH)$_4$** in Ar-sparged MeCN in the presence of 0.13 M AcOH demonstrated that the onset potential of background proton reduction occurs at a ~300 mV more negative potential than the CV observed for the same solution in the presence of O_2 (Fig. 2).

2.2.3. Homogeneous electrochemical ORR using other acids

ORR reactivity studies were performed for **CoTPF$_8$(OH)$_2$** and **CoTPF$_8$(OH)$_4$** using three different Brönsted acids, TFA (pK_a = 12.65), AcOH (pK_a = 23.51), and MeOH (pK_a = 37.44) at 0.13 M in MeCN (Fig. 3A and Fig. S15). The onset potential of the catalytic wave obtained for **CoTPF$_8$(OH)$_2$** maintained a correlation of 40 mV/pK_a, suggesting a rate-determining step involved with $1e^-$ and $1H^+$ (Fig. 3B) [24]. However, a similar analysis for **CoTPF$_8$(OH)$_4$** revealed a slope of 28 mV/pK_a, suggesting $2e^-$ and $1H^+$ transfer at the rate-limiting step that also could favor a faster ORR process [25]. We believe that the additional peak observed for **CoTPF$_8$(OH)$_2$** at −0.3 V is a pre-catalytic wave that is typically observed when the catalyst-substrate adduct is stabilized through H-bonding from the pendant proton relay group [23].

2.2.4. RRDE voltammetry for homogeneous ORR

To benchmark the selectivity of the homogeneous ORR, we carried out rotating ring-disk electrochemistry (RRDE) studies in O_2-saturated MeCN in the presence of 0.13 M AcOH using the procedures described by Nocera et al. [3]. A low concentration of **CoTP(OH)$_2$**, **CoTPF$_8$(OH)$_2$**, and **CoTPF$_8$(OH)$_4$** (1.0 mM) was used for these measurements to maintain an overall pseudo-first order reaction with regard to the dissolved O_2 concentration (~ 8.1 mM in MeCN) [3]. The Faradaic efficiency for H_2O was then calculated using the following equation, Eq. (1) [3,5]:

$$100\text{–}\%H_2O_2 = 100\text{–}\left(\frac{2\ xI_r/N}{I_d + I_r/N}\quad x100\right) \tag{1}$$

where I_r is the ring current, I_d is the disk current, and N is the collection efficiency (= 0.2). The maximum FE for H_2O using **CoTP(OH)$_2$**, **CoTPF$_8$(OH)$_2$**, and **CoTPF$_8$(OH)$_4$** are obtained as 26 %, 92 %, and 97 %, respectively, within the applied potentials closest to the onset potentials, between – 0.5 V and – 1.5 V vs. Fc/Fc^+ (Fig. 4 and Figs. S17–S18).

2.2.5. FOWA and reaction orders

FOWA was performed to gain kinetic insights into the ORR process of **CoTPF$_8$(OH)$_2$**. In O_2-saturated MeCN, **CoTPF$_8$(OH)$_2$** demonstrated quasi-plateau current densities at varied AcOH concentrations ranging from 0.04 M to 0.13 M AcOH (Fig. 5). These CVs were then fitted using the FOWA equation (Fig. 5), and the slopes obtained from FOWA produced the pseudo-first-order reaction rate constants (k_{FOWA}), which can provide the maximum turnover frequency at a given acid concentration

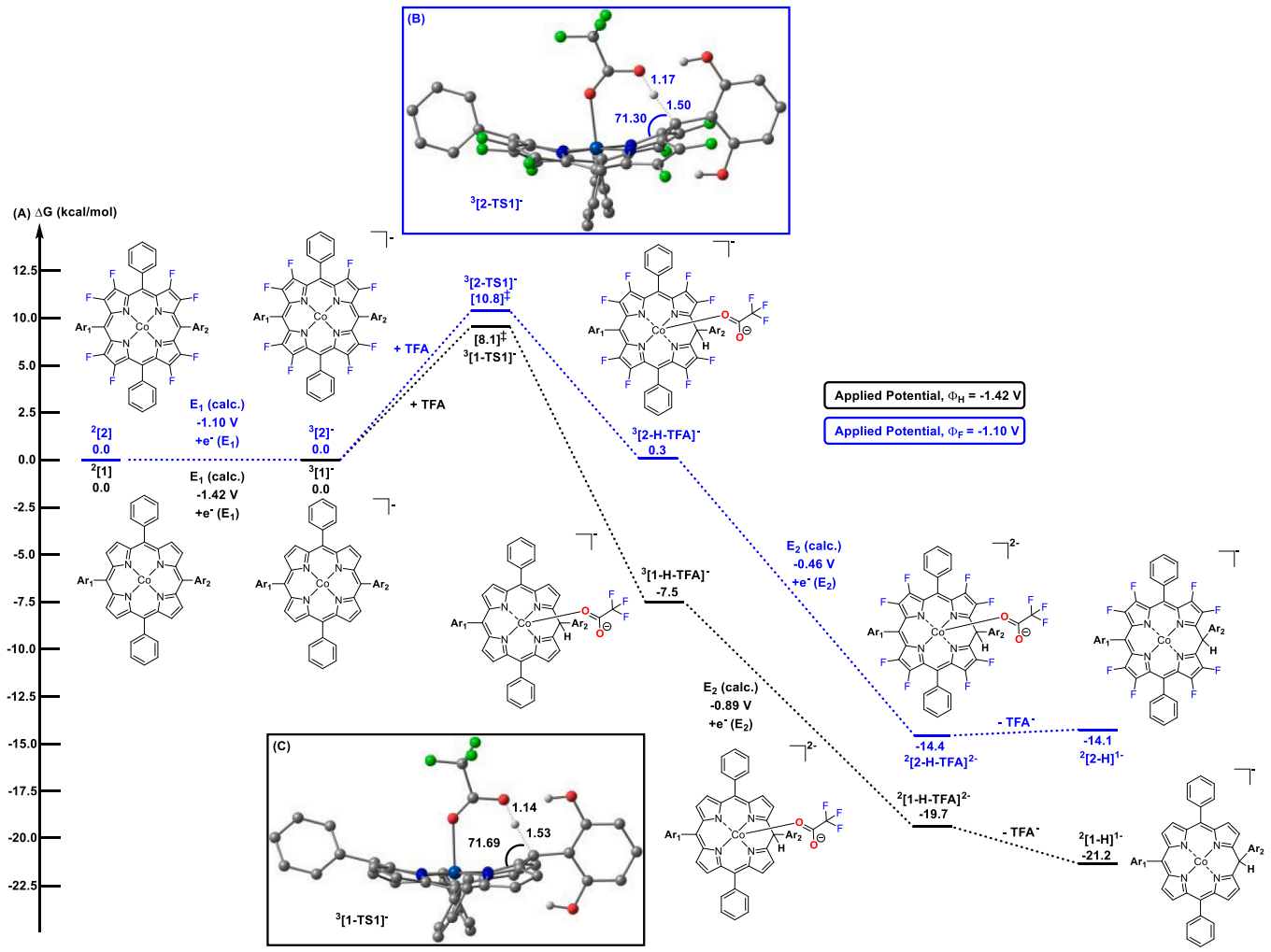

Fig. 6. (A) Computed Gibbs free energy profile (kcal/mol) for forming the monoanionic cobalt phlorin intermediates **[1-H]**$^-$ and **[2-H]**$^-$ in the presence of TFA as the proton source. The computed redox potentials for obtaining the one-electron reduced complexes **[1]**$^-$ and **[2]**$^-$ were used as applied potential. The left superscript represents the spin multiplicity of a given species, while the right superscript is the charge of the overall complex. (B) Transition state for the meso-carbon protonation for the β-substituted catalyst in the presence of TFA. (C) Transition state for the meso-carbon protonation for the non-β-substituted catalyst in the presence of TFA. Distances are in angstroms (Å), and the bond angle is in degrees (°). Non-participating hydrogen atoms are omitted for clarity.

[26]. When the concentrations of catalyst (1.5 mM) and O_2 (8.1 mM in MeCN) were held constant, the logarithms of these k_{FOWA} values were plotted vs. the logarithm of AcOH concentration and fitted linearly, and the slope obtained from the linear fit suggests a first-order reaction with respect to the acid concentration. This first-order reaction suggests that the initial protonation step at the cobalt-superoxide complex involves one equiv. of AcOH, which promotes the generation of the cobalt-hydroperoxo intermediate.

3. Computational investigation of ORR mechanism

Density functional theory (DFT) calculations were employed to probe the ORR mechanism using **$CoTP(OH)_2$ [1]** and **$CoTPF_8(OH)_2$ [2]**, as well as to understand the role of fluorine on the β-positions of the porphyrin macrocycle. Electronic structure calculations indicate that **[1]** and **[2]** have a doublet ground state, consistent with a cobalt(II) center (i.e., the Mulliken spin for cobalt, $\rho_{Co} = 1.1$, d^7, Tables S1 and S2).

The one-electron reduced species were then optimized to determine the computed redox potentials and found to be – 1.42 V vs. Fc/Fc^+ and – 1.10 V vs. Fc/Fc^+, respectively, for **[1]**$^-$ and **[2]**$^-$ (Fig. 6). These reduction potentials, which agree with the experimental data, suggest that **[1]**$^-$ and **[2]**$^-$ have a triplet ground state (Tables S3 and S4). In this regard, the Mulliken spin on cobalt remains unchanged, indicating that the reduction is ligand-based. We note that the more positive redox potential for **[2]**$^-$ is attributed to the electron-withdrawing fluorine groups on the porphyrin ligand, thus lowering the ligand π* orbitals.

Following the formation of the one-electron reduced species, we considered two pathways for ORR. The first involved direct O_2 binding, while the second reaction mechanism began with the meso-carbon protonation of the porphyrin ring in the presence of TFA (i.e., the most acidic proton source in this study, $pK_a = 12.65$). The latter mechanism, which yields a phlorin intermediate, was proposed by Hammes-Schiffer, Nocera, and co-workers for the hydrogen evolution reaction using Hangman Co and Ni porphyrins [27,28]. As shown in Figs. 6 and S21, the formation of the phlorin intermediates **[1-H]**$^-$ and **[2-H]**$^-$ is kinetically accessible under the experimental conditions, but more importantly, **[1-H]**$^-$ and **[2-H]**$^-$ are thermodynamically more favorable than direct O_2 binding to give **[1-O_2]**$^-$ and **[2-O_2]**$^-$ ($\Delta G = -10.5$ and –6.7 kcal/mol, respectively, Fig. S21). Thus, we hypothesized that initial protonation of the meso-carbon of the porphyrin ring to yield a phlorin intermediate could occur before forming the cobalt-superoxide intermediate.

As shown in Fig. 6, the protonation of the meso-carbon is kinetically accessible for both catalysts. For instance, the activation energy for the non-β-substituted complex is 8.1 kcal/mol with respect to the separated reactants, which is 2.7 kcal/mol lower in energy than for **[2]**$^-$. The

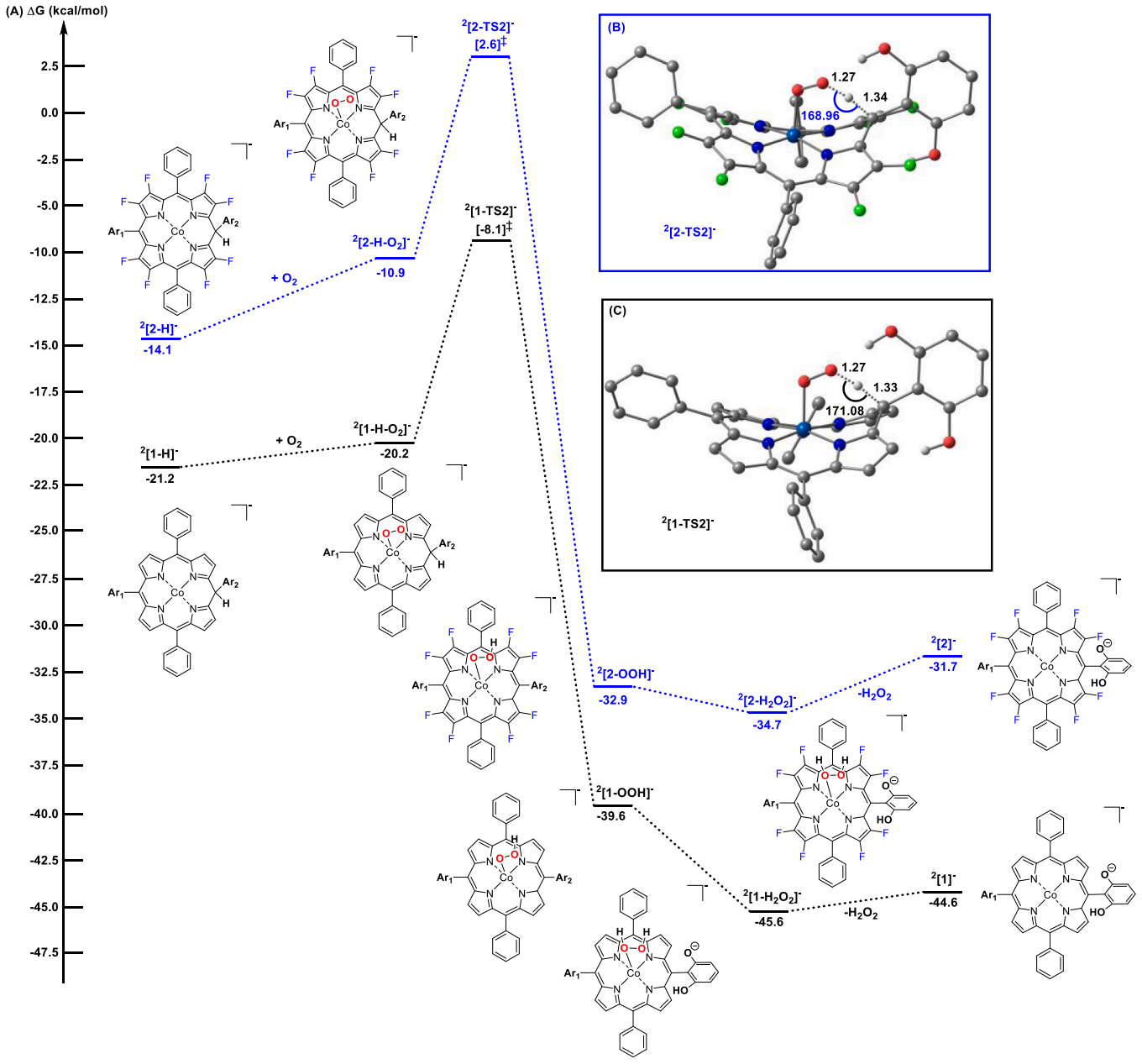

Fig. 7. (A) Computed Gibbs free energy profile (kcal/mol) for forming the cobalt-hydroperoxo species, **[1-OOH]**$^-$ and **[2-OOH]**$^-$, as well as the cobalt-hydroperoxide intermediates **[1-H$_2$O$_2$]**$^-$ and **[2-H$_2$O$_2$]**$^-$. The left superscript represents the spin multiplicity of a given species, while the right superscript is the charge of the overall complex. (B) Transition state for the protonation of the β-O-atom for the β-substituted catalyst. (C) Transition state for the protonation of the β-O-atom for the non-β-substituted catalyst. Distances are in angstroms (Å), and the bond angle is in degrees (°). Non-participating hydrogen atoms are omitted for clarity.

computed bond interactions in **[1-TS1]**$^-$ and **[2-TS1]**$^-$ indicate that the proton from the TFA molecule is fully dissociated (i.e., O···H: 1.14 Å in **[1-TS1]**$^-$ *cf.* 1.17 Å in **[2-TS1]**$^-$) as the meso-carbon gets protonated (i.e., H···C: 1.53 Å in **[1-TS1]**$^-$ *cf.* 1.50 Å in **[2-TS1]**$^-$). Again, the presence of electron-withdrawing fluorine groups on the porphyrin is responsible for such a difference in activation energies.

After forming the phlorin intermediates **[1-H-TFA]**$^-$ and **[2-H-TFA]**$^-$, dissociation of trifluoroacetate is required to create a vacant site at the metal center for O_2 binding. This step was computed to be accessible following a second reduction event at – 0.89 V and – 0.46 V for **[1-H-TFA]**$^-$ and **[2-H-TFA]**$^-$, respectively. Indeed, reduction of **[1-H-TFA]**$^-$ and **[2-H-TFA]**$^-$ facilitate the dissociation of the trifluoroacetate molecule, which is downhill by 1.5 kcal/mol for **[1-H-TFA]**$^-$ and slightly uphill by 0.3 kcal/mol for **[2-H-TFA]**$^-$, yielding, respectively, the phlorin intermediates **[1-H]**$^-$ and **[2-H]**$^-$.

Once the phlorin intermediates **[1-H]**$^-$ and **[2-H]**$^-$ were formed, we hypothesized that O_2 binding could occur (Fig. 7). Although the process is slightly uphill for both compounds, the formation of **[1-H-O$_2$]**$^-$ and **[2-H-O$_2$]**$^-$ facilitated the transfer of the proton from the meso-carbon to the superoxide, through the transition states **[1-TS2]**$^-$ and **[2-TS2]**$^-$ respectively. The computed bond interactions in **[1-TS2]**$^-$ and **[2-TS2]**$^-$ are consistent with the proton transfer (i.e., C···H: 1.33 Å and H···O: 1.27 Å in **[1-TS2]**$^-$ *cf.* C···H: 1.34 Å and H···O: 1.27 Å in **[2-TS2]**$^-$), which yield the cobalt-hydroperoxo species, **[1-OOH]**$^-$ and **[2-OOH]**$^-$. After yielding **[1-OOH]**$^-$ and **[2-OOH]**$^-$, our electronic structure calculations indicated that the cobalt-hydroperoxide intermediates **[1-H$_2$O$_2$]**$^-$ and **[2-H$_2$O$_2$]**$^-$ are thermodynamically more stable than **[1-OOH]**$^-$ and **[2-OOH]**$^-$ by 6.0 kcal/mol and 1.8 kcal/mol, respectively

(Fig. 7). We attempted to locate the transition states for the proton transfer from diol to give the cobalt-hydroperoxide intermediates, and our results suggested that the process was barrierless. This indicates that following the protonation of the cobalt-superoxide, the formation of the cobalt-hydroperoxide intermediates is facile.

After the formation of **[1-H_2O_2]$^-$** and **[2-H_2O_2]$^-$**, the release of H_2O_2 to give the monoanionic **[1]$^-$** and **[2]$^-$** compounds with a deprotonated diol is uphill in nature by 1.0 kcal/mol and 3.0 kcal/mol, respectively (Fig. 7). Furthermore, we note that the formation and release of H_2O_2 from the cobalt-hydroperoxo species, **[1-OOH]$^-$** and **[2-OOH]$^-$** is, respectively, downhill by 5.0 kcal/mol and uphill by 1.2 kcal/mol. These results suggest that due to the weaker binding of hydrogen peroxide in **[1-H_2O_2]$^-$**, H_2O_2 can dissociate. In contrast, the stronger binding of H_2O_2 in **[2-H_2O_2]** allowed further reductions and protonation of the cobalt-hydroperoxide intermediates to generate H_2O, consistent with the experimental observations and the RRDE data for **CoTPF$_8$(OH)$_2$** (Fig. 4).

4. Conclusions

Cobalt-based β-fluorinated porphyrin complexes (**CoTPF$_8$(OH)$_2$** and **CoTPF$_8$(OH)$_4$**) were synthesized, characterized, and investigated for homogeneous electrochemical O_2 reduction. The catalysts, **CoTPF$_8$(OH)$_2$** and **CoTPF$_8$(OH)$_4$**, showed maximum Faradaic efficiency for H_2O of 92 % and 97 %, respectively. In contrast, the non-β-substituted complex analog, **CoTP(OH)$_2$**, was comparatively less selective than the primary β-fluorinated porphyrin complexes analyzed in this study. Based on mechanistic studies, a first-order rate constant with respect to the acid concentration was observed, thereby implying that the initial protonation step at the cobalt-superoxide complex involves one equivalent of AcOH. DFT calculations suggested that phlorin intermediates, as proposed by Hammes-Schiffer, Nocera, and co-workers for the hydrogen evolution reaction using Hangman Co and Ni porphyrins [27,28], could be involved before O_2 reduction. More importantly, electronic structure calculations indicated that the stronger binding of H_2O_2 in the cobalt-based β-fluorinated porphyrin species compared to the parent compound was responsible for the observed experimental selectivity for H_2O. Our findings and mechanistic interpretations demonstrate that incorporating fluorine on the β-positions in cobalt porphyrins gives rise to a selective four-electron reduction of O_2.

CRediT authorship contribution statement

Jianbing Jiang: Writing – review & editing, Writing – original draft, Conceptualization. **Julien Panetier:** Writing – review & editing, Supervision. **Soumalya Sinha:** Data curation. **Sandeep Dash:** Writing – original draft, Software. **Ashwin Chaturvedi:** Writing – review & editing, Writing – original draft, Data curation.

Declaration of Competing Interest

The authors declare that they have no known competing financial interests or personal relationships that could have appeared to influence the work reported in this paper.

Acknowledgements

This work is supported by the National Science Foundation under Grant no. CHE-2041436.

Appendix A. Supporting information

Supplementary data associated with this article can be found in the online version at doi:10.1016/j.mtcata.2024.100053.

References

[1] E.I. Solomon, S.S. Stahl, Introduction: oxygen reduction and activation in catalysis, Chem. Rev. 118 (2018) 2299–2301.
[2] W. Zhang, W. Lai, R. Cao, Energy-related small molecule activation reactions: oxygen reduction and hydrogen and oxygen evolution reactions catalyzed by porphyrin- and corrole-based systems, Chem. Rev. 117 (2017) 3717–3797.
[3] G. Passard, D.K. Dogutan, M. Qiu, C. Costentin, D.G. Nocera, Oxygen reduction reaction promoted by manganese porphyrins, ACS Catal. 8 (2018) 8671–8679.
[4] B. Lv, X. Li, K. Guo, J. Ma, Y. Wang, H. Lei, F. Wang, X. Jin, Q. Zhang, W. Zhang, R. Long, Y. Xiong, U.-P. Apfel, R. Cao, Controlling oxygen reduction selectivity through steric effects: electrocatalytic two-electron and four-electron oxygen reduction with cobalt porphyrin atropisomers, Angew. Chem. Int. Ed. 60 (2021) 12742–12746.
[5] S. Sinha, M. Ghosh, J.J. Warren, Changing the selectivity of O_2 reduction catalysis with one ligand heteroatom, ACS Catal. 9 (2019) 2685–2691.
[6] S. Yoshikawa, A. Shimada, Reaction mechanism of cytochrome c oxidase, Chem. Rev. 115 (2015) 1936–1989.
[7] J.P. Collman, Functional analogs of heme protein active sites, Inorg. Chem. 36 (1997) 5145–5155.
[8] J.P. Collman, N.K. Devaraj, R.A. Decréau, Y. Yang, Y.-L. Yan, W. Ebina, T. A. Eberspacher, C.E.D. Chidsey, A cytochrome c oxidase model catalyzes oxygen to water reduction under rate-limiting electron flux, Science 315 (2007) 1565–1568.
[9] S. Fukuzumi, S. Mandal, K. Mase, K. Ohkubo, H. Park, J. Benet-Buchholz, W. Nam, A. Llobet, Catalytic four-electron reduction of O_2 via rate-determining proton-coupled electron transfer to a dinuclear cobalt-μ-1,2-peroxo complex, J. Am. Chem. Soc. 134 (2012) 9906–9909.
[10] G. Passard, A.M. Ullman, C.N. Brodsky, D.G. Nocera, Oxygen reduction catalysis at a dicobalt center: the relationship of Faradaic efficiency to overpotential, J. Am. Chem. Soc. 138 (2016) 2925–2928.
[11] Y. Liu, G. Zhou, Z. Zhang, H. Lei, Z. Yao, J. Li, J. Lin, R. Cao, Significantly improved electrocatalytic oxygen reduction by an asymmetrical pacman dinuclear cobalt(II) porphyrin–porphyrin dyad, Chem. Sci. 11 (2020) 87–96.
[12] I. Monte-Pérez, S. Kundu, A. Chandra, K.E. Craigo, P. Chernev, U. Kuhlmann, H. Dau, P. Hildebrandt, C. Greco, C. Van Stappen, N. Lehnert, K. Ray, Temperature dependence of the catalytic two- versus four-electron reduction of dioxygen by a hexanuclear cobalt complex, J. Am. Chem. Soc. 139 (2017) 15033–15042.
[13] P.T. Smith, Y. Kim, B.P. Benke, K. Kim, C.J. Chang, Supramolecular tuning enables selective oxygen reduction catalyzed by cobalt porphyrins for direct electrosynthesis of hydrogen peroxide, Angew. Chem. Int. Ed. 59 (2020) 4902–4907.
[14] X. Li, P. Li, J. Yang, L. Xie, N. Wang, H. Lei, C. Zhang, W. Zhang, Y.-M. Lee, W. Zhang, S. Fukuzumi, W. Nam, R. Cao, A cobalt(II) porphyrin with a tethered imidazole for efficient oxygen reduction and evolution electrocatalysis, J. Energy Chem. 76 (2023) 617–621.
[15] R.R. Durand, F.C. Anson, Catalysis of dioxygen reduction at graphite electrodes by an adsorbed cobalt(II) porphyrin, J. Electroanal. Chem. Interfacial Electrochem 134 (1982) 273–289.
[16] E. Song, C. Shi, F.C. Anson, Comparison of the behavior of several cobalt porphyrins as electrocatalysts for the reduction of O_2 at graphite electrodes, Langmuir 14 (1998) 4315–4321.
[17] C. Shi, F.C. Anson, 5,10,15,20-Tetramethylporphyrinato)cobalt(II): a remarkably active catalyst for the electroreduction of O_2 to H_2O, Inorg. Chem. 37 (1998) 1037–1043.
[18] R. Zhang, J.J. Warren, Controlling the oxygen reduction selectivity of asymmetric cobalt porphyrins by using local electrostatic interactions, J. Am. Chem. Soc. 142 (2020) 13426–13434.
[19] E.K. Woller, S.G. DiMagno, 2,3,7,8,12,13,17,18-Octafluoro-5,10,15,20-tetraarylporphyrins and their zinc complexes: first spectroscopic, electrochemical, and structural characterization of a perfluorinated tetraarylmetalloporphyrin, J. Org. Chem. 62 (1997) 1588–1593.
[20] M.-S. Liao, J.D. Watts, M.-J. Huang, Effects of peripheral substituents and axial ligands on the electronic structure and properties of cobalt porphyrins, J. Phys. Chem. A 109 (2005) 11996–12005.
[21] C. Kashi, C.-C. Wu, C.-L. Mai, C.-Y. Yeh, C.K. Chang, Synthesis of octafluoroporphyrin, Angew. Chem. Int. Ed. 55 (2016) 5035–5039.
[22] N. Elgrishi, K.J. Rountree, B.D. McCarthy, E.S. Rountree, T.T. Eisenhart, J. L. Dempsey, A practical beginner's guide to cyclic voltammetry, J. Chem. Educ. 95 (2017) 197–206.
[23] S. Sinha, L.M. Mirica, Electrocatalytic O_2 reduction by an organometallic Pd(III) complex via a binuclear Pd(III) intermediate, ACS Catal. 11 (2021) 5202–5211.
[24] J.Bard Allen, R.Faulkner Larry, Electrochemical Methods: Fundamentals and Applications, 2nd Ed, Wiley, New York, 2001 (Russian Journal of Electrochemistry 2002, 38, 1364–1365).
[25] M.L. Pegis, D.J. Martin, C.F. Wise, A.C. Brezny, S.I. Johnson, L.E. Johnson, N. Kumar, S. Raugei, J.M. Mayer, Mechanism of catalytic O_2 reduction by iron tetraphenylporphyrin, J. Am. Chem. Soc. 141 (2019) 8315–8326.
[26] C. Costentin, J.-M. Savéant, Multielectron, multistep molecular catalysis of electrochemical reactions: benchmarking of homogeneous catalysts, ChemElectroChem 1 (2014) 1226–1236.
[27] B.H. Solis, A.G. Maher, T. Honda, D.C. Powers, D.G. Nocera, S. Hammes-Schiffer, Theoretical analysis of cobalt hangman porphyrins: ligand dearomatization and mechanistic implications for hydrogen evolution, ACS Catal. 4 (2014) 4516–4526.
[28] B.H. Solis, A.G. Maher, D.K. Dogutan, D.G. Nocera, S. Hammes-Schiffer, Nickel phlorin intermediate formed by proton-coupled electron transfer in hydrogen evolution mechanism, Proc. Natl. Acad. Sci. USA 113 (2016) 485–492.